RESIDUAL STRESS AND TORSIONAL BUCKLING STRENGTH OF H AND CRUCIFORM COLUMNS

By Fumio Nishino, Lambert Tall** and Toshie Okumura****

ABSTRACT

The torsional buckling strength of axially loaded H and cruciform columns is studied with particular attention given to the effect of residual stress. A numerical approach was used in evaluating the torsional buckling strength so that columns with various patterns of residual stress distribution could be analysed. A series of five welded built-up cruciform columns of constructional alloy steel have been tested and compared with theoretical results.

The results of this study indicate that the width-thickness ratio of an outstanding flange made of constructional alloy steel should be limited to 7.5 in order to avoid premature torsional failure.

1. INTRODUCTION

Residual stresses were introduced in the past decade as the main factor influencing the flexural buckling strength of centrally loaded columns defined by the Euler load and the yield load.

The torsional buckling strength of a steel column is regarded, generally, as being far above the buckling strength in bending so that the torsional buckling normally does not need to be considered[1]. The recent progress in steel making, however, has resulted in the production of extremely high strength steel. It seems possible that the difference between the torsional and the bending buckling strength of a column with open cross section may become insignificant when the static yield stress of the material becomes higher, when the same geometry is retained. Further, for the cross section of a column which does not have two axes of symmetry, the torsional buckling and the flexural buckling can not be divided into two different phenomena. Under these conditions, it was felt worthwhile to consider the effect of residual stresses on the torsional buckling strength of a steel column.

* Associate Professor, Structural Testing Laboratory, Engineering Research Institute, University of Tokyo, Tokyo, Japan.

** Associate Professor of Civil Engineering, Chairman, Structural Metals Division, Fritz Engineering Laboratory, Lehigh University, Bethlehem, Pennsylvania, U.S.A.

*** Professor of Civil Engineering, University of Tokyo, Tokyo, Japan.

The study of inelastic torsional buckling was not considered much in the past. A study has been made by Stowell[2] on the inelastic buckling of hinged flanges, where the theory of inelastic buckling of plates was applied, rather than column theory. The inelastic torsional buckling topic was given more attention in the field of beams and beam-columns, where lateral or lateral-torsional buckling was the major cause of failure. The solutions for lateral and lateral-torsional buckling were obtained for wide-flange beams and beam-columns of structural carbon steel in the inelastic range[3),4),5),6)].

In the field of aeronautical engineering, the influence of aerodynamic heating on torsional stiffness had been gaining attention in recent years. Several investigators have shown that thermal stress reduced the torsional stiffness of the wings[7),8),9)]. The behavior of a section containing residual stresses may be similar to one containing uneven thermal stresses. In view of this, these studies can be considered as closely related to the study of torsional buckling with residual stress.

A paper has been presented discussing the effect of residual stress on the flexural-torsional buckling of steel columns[10], in which it was shown theoretically as well as experimentally that residual stresses have a marked effect on elastic buckling as well as on inelastic buckling of angle and cruciform columns. Recently, a paper was presented which dealt the effect of residual stress on torsional buckling strength of rolled wide-flange H-columns[11]. In the paper, however, a misunderstanding of the problem seems to be present[12),13)] and applicability of the numerical results to a wide flange column may be questionable. A paper is available on the local buckling of a flange plate of plate girders with consideration of the effect of residual stress[14]. The paper deals essentially with torsional instability of an outstanding flange elastically supported at one of the unloaded edges, and thus the work is closely related to the torsional buckling strength of a steel column. All of the three papers employed an analytical approach in evaluating the stress distribution and the stiffnesses of the cross sections and thus the results obtained were applicable only to columns of a particular material and manufacturing process. In this paper, a numerical approach is employed in the

analysis and the buckling strengths of higher strength steel are numerically examined. The results are compared with tests of cruciform columns of quenched and tempered constructional alloy steel.

The theoretical part of the paper is based on a dissertation[15] to which reference may be made for detailed information. Some extracts of the dissertation were presented in a journal[16] to which reference is also made.

2. BUCKLING STRENGTHS OF COLUMNS

2.1 Assumptions

In the analysis of this paper, only columns with open cross section and which are constant along the length are considered. The column is assumed to be long enough that distribution of residual stress is constant along its length for practical purposes. The main object of the study is to investigate the effect of residual stress on the buckling strength of a centrally loaded column. The residual stress affects the buckling strength from two reasons; one is the non-uniform stress distribution and the other is partial yielding of the cross section. For a column with residual stress, the stress present at any point in the cross section is no longer uniform even for a column axially loaded at the centroid and the stress σ may be expressed as

$$\sigma=\sigma_0+\sigma_r \quad \cdots\cdots(1)$$

provided no yielding penetrates the cross section. σ_0 is the uniform stress due to external loading at the centroid and the magnitude is equal to the load P divided by the cross sectional area A. σ_r is the magnitude of residual stress present at the point prior to the application of the external load. With the increase of the external loading, the stress reaches the yield stress of the material and yielding starts to penetrate from a point where the maximum compressive residual stress was present. With the penetration of yielding, the rigidity of the material at that part reduces, which in turn reduces the overall stiffness of the cross section. This reduction is due to the presence of residual stress in the case of a centrally loaded column. Numerous measurements on the residual stresses present in structural steel plates and shapes were made and the results are available in the literature[17),18),19),20]. Although the measured patterns of the residual stress are not always symmetric, it is assumed that distribution of residual stress is symmetric about an axis of symmetry of the cross section. With this assumption, the stress distribution as well as the penetration of partial yielding become symmetric for any axis of symmetry.

The residual stress in a cross section is in self-equilibrium and thus, in performing numerical computation, it has to satisfy the following conditions of statics ; no resulting axial force, no resulting bending moments on two principal axes, and no resulting twisting moment. The first condition is obvious. The conditions on bending moments are satisfied automatically with the above assumption for a cross section with two axes of symmetry, however a difficulty arises in the analysis of a column with a cross section with single axis of symmetry or without any axis of symmetry. With the assumption of constant distribution of residual stress along the length of a column, it is easily shown that no residual shear is present, and therefore the condition on twisting moment is automatically satisfied. Lee *et al.* introduced in their paper[11] the condition on twisting moment in the form of

$$\int_A \sigma_r(x^2+y^2)dA=0 \quad \cdots\cdots(2)$$

The condition imposes a further restriction on the residual stress distribution, resulting in no reduction of elastic buckling strength due to the presence of residual stress. Discussions on this condition have been raised[12),13)].

2.2 Buckling Equation

The differential equation of torsional equilibrium is written as follows for a column with doubly symmetric cross section[11),15)]

$$C_w\frac{d^4\phi}{dz^4}+\left[\int_A\sigma(x^2+y^2)dA-C_t\right]\frac{d^2\phi}{dz^2}=0 \quad \cdots(3)$$

where C_w is the warping rigidity and C_t is the St. Venant's torsional rigidity. The conditions of a column for which the equation of equilibrium is applicable are;

(1) doubly symmetric cross section for geometry and for material properties,

(2) doubly symmetric distribution of residual stress in a section, and

(3) all of the above properties constant along the whole length.

A column with a doubly symmetric distribution of residual stress in a section and constant distribution along the length as assumed earlier satisfies the above conditions, and therefore the equation can be used in the buckling analysis of the column for elastic buckling as well as for buckling after partial yielding has penetrated the cross section.

The buckling equation can be obtained as in literature[21] for a simply supported column at both ends for bending as well as for twisting and the equation is written as;

$$\frac{\pi^2}{L^2}C_w+C_t-\int_A\sigma(x^2+y^2)dA=0 \quad \cdots\cdots(4)$$

Substituting Eq. 1 into the above equation and rewriting the equation using the relationship $\sigma_0=P_{cr}/A$, the following expression for the elastic buckling load is obtained

$$P_{cr}=\frac{I_p}{A}\left[\frac{\pi^2}{L^2}C_w+C_t-\int_A\sigma_r(x^2+y^2)dA\right] \quad (5)$$

For a column free of residual stress, σ_r in Eq. 5 is

equal to zero and the buckling load is expressed as

$$P_{cr}=\frac{I_p}{A}\left(\frac{\pi^2}{L^2}C_w+C_t\right) \quad \cdots\cdots(6)$$

and the expression coincides with the well known expression for the torsional buckling strength[21].

The last term in Eq. 5 is not always equal to zero and therefore it is obvious that the presence of residual stress affects the buckling strength even for elastic buckling*.

Under the assumption that no strain reversal takes place at the instant of buckling, the warping rigidity of a cross section can be expressed as[15]

$$C_w=\int E_t W_n t\,ds \quad \cdots\cdots(7)$$

where W_n is the unit warping[1),21)] of the cross section. The stress-strain relationship of structural steel is close to that of the elastic-perfectly-plastic material. For a steel column with an elastic-perfectly-plastic stress-strain relationship, the expression for the warping rigidity is simplified as

$$C_w=EI_{we} \quad \cdots\cdots(8)$$

where E is the modulus of elasticity and I_{we} is the warping constant of the elastic portion of the cross section with respect to the original shear center. St. Venant's torsional rigidity for an elastic thin-walled open cross section is defined by

$$C_t=G\int\frac{t^3}{3}ds \quad \cdots\cdots(9)$$

where G is the modulus of elasticity in shear and t is the thickness of the plate elements. For the yielded portion of the cross section, two basic theories, which were applied to the buckling analysis of aluminum alloy plates, exist for the shearing rigidity. One is the so-called incremental theory[22] and the other is the total strain theory[23].

Imposing the requirement that the stress condition is uniaxial prior to buckling and no strain reversal takes place at the instant of buckling, the total strain theory by Bijlaard[23] predicts the following shearing modulus

$$G_t=\frac{E}{2+2\nu+3e} \quad \cdots\cdots(10)$$

where ν is the Poisson's ratio and e is the ratio of plastic strain to elastic strain, ϵ_p/ϵ_Y. A loss of strain in the strain history, which is the main assumption of the incremental theory, amounts only to a neglect of the initial plastic deformation at the instant of buckling, which is taken into account by equating e to zero. As a consequence, the incremental theory predicts the same torsional rigidity for the yielded portion as that of elastic portion. The shearing modulus is not clear yet; however, if it is expressed by G_t at the instant of buckling, the Saint Venant's torsional rigidity can be determined as

$$C_t=\int G_t\frac{t^3}{3}ds \quad \cdots\cdots(11)$$

2.3 Numerical Evaluation of Buckling Strength

In the solution of the buckling strength of a column loaded into the inelastic range, it is not, in general, practical to solve for the buckling load, but it is easier to solve for the critical length under a known loading. Equation 4 can be solved for the critical length of a column which buckles under a loading P:

$$L=\pi\sqrt{\frac{C_w}{\int_A\sigma(x^2+y^2)\,dA-C_t}} \quad \cdots\cdots(12)$$

The buckling load versus the critical length relationship can be determined from the above equation together with the loading P determined by

$$P=\int_A\sigma\,dA \quad \cdots\cdots(13)$$

The determination of the buckling load versus the critical length relationship is, then, merely the evaluation of the stiffnesses C_w and C_t and stress distribution σ in Eq. 12. The analytical approach was preferred in the past[10),11),14)], however, a numerical approach is used in this study so that any pattern of residual stress distribution can be included with much less effort in the analysis as well as in the programming for a digital computer.

As an example of numerical evaluation, the torsional buckling of H-shaped columns is considered. The cross section of an H-column is considered as consisting of small segments; $2n$ segments for a flange and $2m$ segments for the web as shown in Fig. 1, where the dimensions of the cross section and other notations are given. The segment may be small enough so that the variation of magnitude of residual stress can be assumed to be linear inside the segments in the direction of the width of a plate element and constant in the thickness direction of the thin-plate elements. The assumption makes the required numerical integration over the cross section

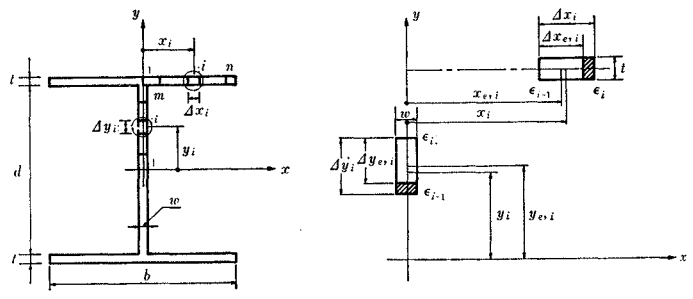

(a) Dimension of Cross Section (b) Detail of Segments

Fig. 1 Dimensions of H-Section.

* This was first pointed out in Ref. 10.

easier.

With an uniformly distributed strain because of external loading and a given distribution of residual strains at the boundaries of the segments, the strain distribution inside each segment is known, and consequently, the stress distribution and the penetration of yielding inside the segment can be determined.

The strains ϵ_{i-1} and ϵ_i at the edges of the segment at the instant of buckling are

$$\left.\begin{aligned}\epsilon_{i-1}&=\epsilon_{r,i-1}+\epsilon_{cr}\\ \epsilon_i&=\epsilon_{r,i}+\epsilon_{cr}\end{aligned}\right\} \quad \cdots\cdots(14)$$

where ϵ_{cr} is the strain due to the external load at which the column is going to buckle and ϵ_r is the given residual strain at the edges of the segment. The subscripts i and $i-1$ refer to the values at the both edges of segment i as shown in Fig. 1. The average stress in the segment can be easily obtained from the known strains at the edges with the use of the assumption on the strain distribution inside the segment.

The average stresses are calculated and are listed in the Appendix for various combinations of magnitudes of strains at the edges.

The external load which causes the uniformly distributed strain ϵ_{cr} can be computed from Eq. 13 as the sum of the force acting on each segment and thus

$$P=4\sum_{i=1}^{n}\sigma_i\Delta A+2\sum_{i=1}^{m}\sigma_i\Delta A \quad \cdots\cdots(15)$$

where ΔA is the area of each segment and σ_i is the average stress in the segment i. $\sum_{i=1}^{n}$ and $\sum_{i=1}^{m}$ denote the summations over a half of the flange and the web plates, respectively.

The other terms to be computed for obtaining the critical length of a pinned-end column, are the stiffness coefficients; C_w and C_t and $\int_A\sigma(x^2+y^2)\,dA$, as noted in Eq. 12.

Although the stiffness coefficient C_w can be computed by Eq. 7, it is easier to determine the stiffness C_w as a cross bending stiffness of the cross section. Introducing the tangent modulus of elasticity E_t, the cross bending stiffness of an H-section can be expressed as

$$C_w=\left(\frac{d+t}{2}\right)^2\int_{-b/2}^{b/2}2\left(\frac{E_t}{E}\right)tx^2dx \quad \cdots\cdots(16)$$

Because of the assumed stress-strain relationship of steel, Eq. 16 shows that the resistance of the flanges to cross bending is provided only by the elastic parts of the flange. Then performing the integration in Eq. 16 over each of the segments, the following expression can be obtained in a form of summation of the properties of each segment in the flange

$$C_w=\frac{E(d+t)^2b^2t}{96n^3}\sum_{i=1}^{n}\left(\frac{\Delta X_{e,i}}{\Delta X}\right)\left[12\left(\frac{X_{e,i}}{\Delta X}\right)+\left(\frac{\Delta X_{e,i}}{\Delta X}\right)\right] \quad \cdots\cdots(17)$$

where $X_{e,i}$ is the coordinate at the center of the elastic part of the segment i, of which the width is $\Delta X_{e,i}$, as shown in Fig. 1; both of which are determined by the strains at the edges and are also listed in the Appendix.

Defining the reduction of the shearing modulus due to the penetration of yielding at the inception of buckling as

$$K=\frac{G_t}{G} \quad \cdots\cdots(18)$$

the St. Venant's torsional stiffness can be determined from Eq. 11. A similar integration used for the derivation of Eq. 17 results in the following equation for the stiffness

$$C_t=\frac{G}{3}\left[\frac{2t^3b}{n}\sum_{i=1}^{n}K_i+\frac{w^3d}{m}\sum_{i=1}^{m}K_i\right] \quad \cdots\cdots(19)$$

Where K_i is the averaged value of K at segment i. According to the incremental theory, the average value is equal to unity, while the value based on the total strain theory is determined by performing the following integration

$$K_i=\frac{1}{\Delta s}\int_{(i-1)\Delta s}^{i\Delta s}K\,ds \quad \cdots\cdots(20)$$

where Δs is the width of the segment in the direction of the width of the plate element. The average values of K are summarized in the Appendix for various combinations of edge strains.

The last term to be determined is $\int_A\sigma(x^2+y^2)\,dA$. By the assumption, the stress is constant in the thickness direction of each component plate so that the integration may be made only in one direction, along the mid-line of the plates. Performing the integration over each of the segments with strain changing linearly inside the segments, the term can be expressed in the following form

$$\int_A\sigma(x^2+y^2)\,dA=\frac{w^3d}{12m}\sum_{i=1}^{m}\sigma_i+\frac{2b}{n}\left(\frac{d^2t}{4}+\frac{dt^2}{2}+\frac{t^3}{3}\right)\sum_{i=1}^{n}\sigma_i+\frac{wd^3}{4m^3}\sum_{i=1}^{m}q_i+\frac{tb^3}{2n^3}\sum_{i=1}^{n}q_i \quad \cdots\cdots(21)$$

where q_i is defined by

$$q_i=\frac{1}{\Delta s^3}\int_{(i-1)\Delta s}^{i\Delta s}\sigma s^2ds \quad \cdots\cdots(22)$$

and is also summarized in Appendix.

Substitution of Eqs. 17, 19 and 21 into Eq. 12 results in a critical length of the pinned-end column, which buckles under a load obtained by Eq. 15. By varying the strain, ϵ_{cr}, from a small value to a large value at a certain increment, a complete buckling curve of load versus length of a pinned-end column can be obtained.

3. NUMERICAL EXAMPLES

The numerical computation was carried out by a digital computer for the torsional buckling of H-columns and cruciform columns. Although any

distribution of residual stress can be considered, only idealized patterns of residual stress distribution as shown in Fig. 2 were used for the illustration of the buckling of H-columns. In Fig. 2, σ_{rt} and σ_{rc} are the mean tensile and compressive residual stresses, respectively, and σ_Y is the yield stress. The triangular distribution is close to the patterns found in rolled heat-treated shapes[19], whereas the other pattern resembles the pattern in welded shapes[18),20]. The residual stresses in rolled shapes of structural carbon steels and low alloy high-strength steels are idealized more accurately by a parabolic distribution[17]. The column curve for a parabolic distribution, however, would have characteristics intermediate to the above two cases.

Fig. 3 gives the column curves of stress versus pinned-end column length for the torsional buckling

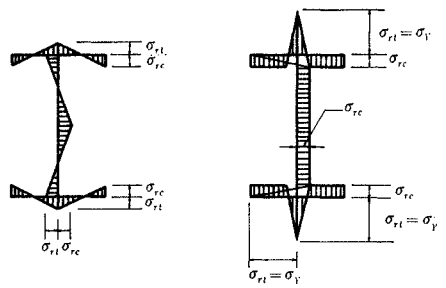

(a) Cooling Pattern (b) Welding Pattern

Fig. 2 Idealized Residual Stress Patterns.

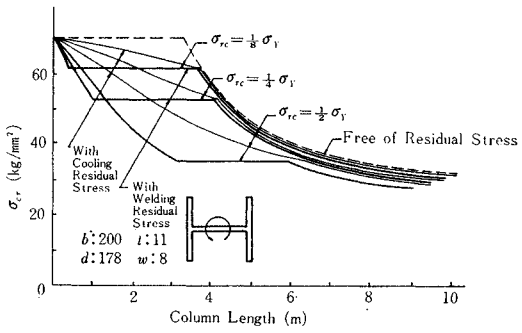

(a) Cross Section : $200\times200\times11\times8$ (8 WF 31) ($\sigma_Y=70$ kg/mm²)

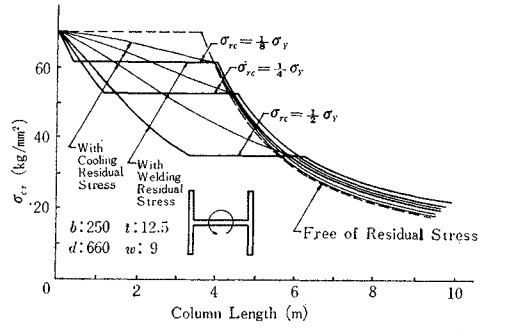

(b) Cross Section : $685\times250\times12.5\times19$ (27 WF 94) ($\sigma_Y=70$ kg/mm²)

Fig. 3 Torsional Buckling Curves of H-Columns.

of the H-columns with cross section of $200\times200\times11\times8$ (8 WF 31) and $685\times250\times12.5\times19$ (27 WF 94) as shown in the figure. Since non-dimensionalization is not easy for torsional buckling, the curves had to be computed for a particular steel; constructional alloy steel with an ultimate tensile strength of 80 kg/mm² was chosen for the illustration, of which the static yield stress was assumed to be 70 kg/mm² with the modulus of elasticity as 2.1×10^6 kg/mm². It is noted that Fig. 3 shows clearly the effect of residual stress on elastic buckling as has been pointed out earlier. With the assumed residual stress distribution, the presence of residual stress reduces the elastic buckling strengths of H-columns of $200\times200\times11\times8$ for any length of the columns. It is of interest to note that the same residual stress distribution raises the elastic buckling strength as seen for H-columns with cross section of $685\times250\times12.5\times19$ in which the effect of tensile residual stress at the junctions of the web and the flange plates and adjacent areas is greater than that of compressive residual stresses at the flange tips because of the property of the cross section, comparatively small flanges and a deep web. The discontinuities of column curves for the sections with welding type residual stress patterns are due to abrupt simultaneous yielding over a large portion of the cross section. For the assumed residual stress patterns of Fig. 2. a the larger the amount of compressive residual stress, the greater the reduction of strength for the entire elastic-plastic buckling. The same is true for the assumed residual stress pattern of Fig. 2. b except for columns of small slenderness ratio. For the same magnitude of the maximum compressive residual stress, the effect of residual stress distribution of the welding type is more pronounced than that of the triangular type. The effect of residual stress in elastic buckling strength, the raising or lowering of buckling strength, is constant for a residual stress distribution regardless of the column length, while the reduction in elastic-plastic buckling depends largely on the column length. Both the incremental and the total strain theories of plasticity resulted in an insignificant difference. This is due to the large contribution of warping rigidity against buckling in the elastic-plastic range of the columns used for the illustration.

The relationship among the three buckling strengths, flexural buckling strengths* about the weak and the strong axes and the torsional buckling strength, is shown in Figs. 4 and 5 in which column curves are drawn for critical stress versus lengths of pinned-end columns. The weakest buckling mode is that of flexural buckling about the weak axis. The torsional buckling strength of $685\times250\times12.5\times19$

* The flexural buckling strengths are computed by a similar method as for the torsional buckling presented in this paper[15].

columns is far smaller than the strong axis buckling strength for the entire length of practical columns. An H-column of constructional alloy steel will most likely fail by torsional instability if failure about the weak axis is prevented. The difference in buckling strengths of torsional failure and weak axis failure would be insignificant in welded H-columns of the steel of lower slenderness ratio as can be seen in Fig. 5; for example, both buckling strengths of the $200\times200\times11\times8$ H-column with the assumed pattern of welding type residual stress are identical, if the pinned-end length of the column is between 1.0 and 3.0 m; the same is true for $685\times250\times12.5\times19$ H-column if the length is between 1.1 and 3.5 m. Thus, the failure mode of these columns might be governed by such factors as unavoidable initial crookedness and eccentricity of loading.

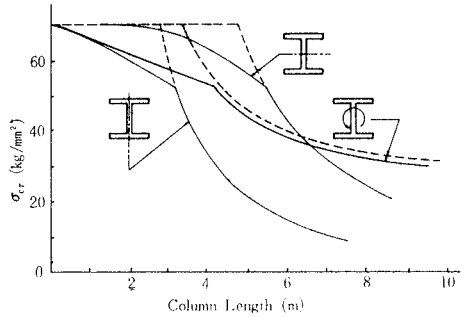

(a) Cross Section : $200\times200\times11\times8$(8 WF 31) ($\sigma_Y$=70 kg/mm²)

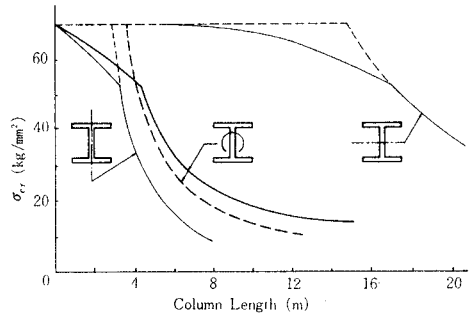

(b) Cross Section : $685\times250\times12.5\times19$(27 WF 94) ($\sigma_Y$=70 kg/mm²)

Fig. 4 Column Curves of Various Buckling Modes (with Cooling Residual Stress : $\sigma_{rc}=1/4\,\sigma_Y$)

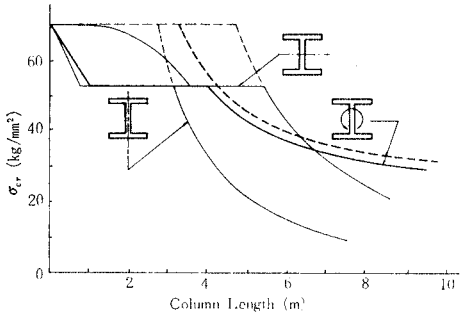

(a) Cross Section : $200\times200\times11\times8$(8 WF 31) ($\sigma_Y$=70 kg/mm²)

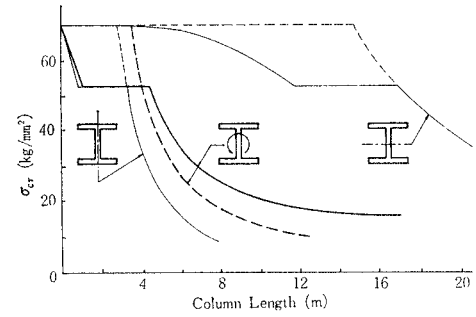

(b) Cross Section : $685\times250\times12.5\times19$(27 WF 94) ($\sigma_Y$=70 kg/mm²)

Fig. 5 Column Curves of Various Buckling Modes (with Welding Residual Stress : $\sigma_{rc}=1/4\,\sigma_Y$)

To illustrate the effect of residual stress on torsional buckling of columns with cross section of relatively smaller warping rigidity, torsional buckling curves were computed for cruciform columns. In the analysis of thin-walled members, it is frequently assumed[21] that no resistance of a plate element is present in the direction perpendicular to the plate. With this assumption, the warping rigidity vanishes for the cross section. The buckling condition, then, becomes as follows by omitting the first term of Eq. 4

$$C_t-\int_A \sigma(x^2+y^2)dA=0 \quad \cdots\cdots\cdots\cdots\cdots\cdots\cdots\cdots(23)$$

Since the cross section is doubly symmetric, it is enough to consider only one of the four flanges in the analysis. The flange is divided into m segments as shown in Fig. 6. The similar operation of Eq. 23 as for H-columns results in the following equation

$$\frac{Gw^3b}{3m}\sum_{i=1}^{m}K_i-\frac{w^3b}{12m}\sum_{i=1}^{m}\sigma_i-\frac{wb^3}{m^3}\sum_{i=1}^{m}q_i=0$$

To be compatible with the assumption of no warping rigidity for the cross section, the second term in the above equation is usually neglected when compared with the third term and thus

$$-\frac{Gw^3b}{3m}\sum_{i=1}^{m}K_i-\frac{wb^3}{m^3}\sum_{i=1}^{m}q_i=0 \quad \cdots\cdots\cdots\cdots\cdots\cdots\cdots\cdots(24)$$

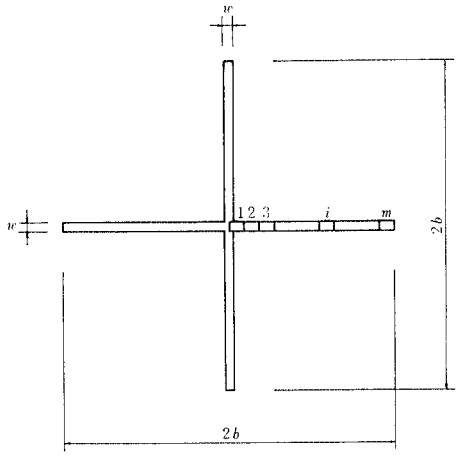

Fig. 6 Dimensions of Cruciform Cross Section.

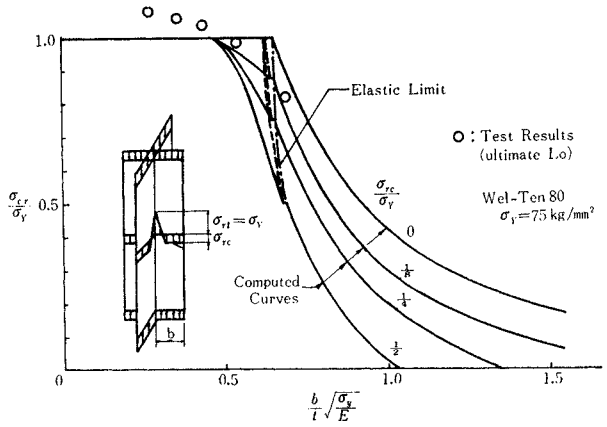

Fig. 7 Torsional Buckling of Cruciform Columns.

The buckling load for a column with this cross section is not a function of the length, instead it is a function of only the dimension of the cross section. The buckling load can be determined by finding the strain ϵ_{cr} which satisfies Eq. 24. The numerical results obtained are presented in Fig. 7 for the residual stress distribution shown in the figure. The ordinate is the buckling stress non-dimensionalized by the yield stress of the material; the abscissa is the width-thickness ratio including a further standardizing factor of $\sqrt{\sigma_Y/E}$ with which the numerical results can be applicable to steel columns regardless of their strength. The assumed residual stress pattern reduces the buckling strength regardless of the width-thickness ratio. The reduction in elastic buckling is rather constant for a residual stress distribution independent of width-thickness ratio. For the elastic-plastic buckling, as opposed to the previous examples of H-columns, a marked difference can be seen due to the difference in the prediction of the shearing rigidity at the instant of buckling, solid lines are the results based on the total strain theory, while the broken lines are the results based on the incremental theory. The reduction of elastic-plastic buckling strength based on the total strain theory depends largely on the width-thickness ratio. It is to be noted that the column curves intersect the horizontal line corresponding to the yield stress of the material. This is one of the basic differences of the torsional buckling of a column compared with the flexural buckling and it comes from the fact that the shearing modulus does not vanish, even an elastic-perfectly-plastic material like steel is compressed to the yield.

4. COMPARISON WITH TEST RESULTS

Experiments have been made in order to correlate with the theoretical analysis. One of the points to be answered through an experimental study is the applicability of the two different predictions of the shearing modulus of elasticity for yielded portion of steel columns.

Since a marked difference is present in the inelastic buckling strength of a cruciform column, the cross section was selected for this experimental study. The experiments consisted of five welded built-up columns made from Wel-Ten 80C steel, a quenched and tempered constructional alloy steel with a minimum guaranteed tensile strength of 80 kg/mm². The nominal size of 5 mm was used in fillet welding of the two flanges on both surfaces of a wider plate to form the cruciform cross section. One of the aim of these tests is to determine experimentally the width-thickness ratio to be used for outstanding flanges made of 80 kg/mm² strength steel, for which no experimental study has been reported; the boundary condition for one flange of an axially loaded cruciform column represents the weakest condition for an outstanding flange. The width-thickness ratio ranged from 4.5 to 11.5 such that the critical loads were reached in both the elastic range and the inelastic range. The lengths of the columns were selected to be eight times the width of the flanges so as not to release the residual stresses.

The yield stress of the steel was determined to be 74.9 kg/mm² from the three tensile tests of standard coupons (gage length 200 mm). The loading was applied continuously with the slowest strain rate possible with the hydraulic testing machine used for the tests. Fig. 8 shows one of the results of stress-strain relationship recorded by an X-Y plotter.

The residual stresses present in the test specimens were measured by "the method of sectioning". The electric wire strain gages of self temperature effect compensating type were attached on both surfaces and the flange tips at one cross section at a sufficient

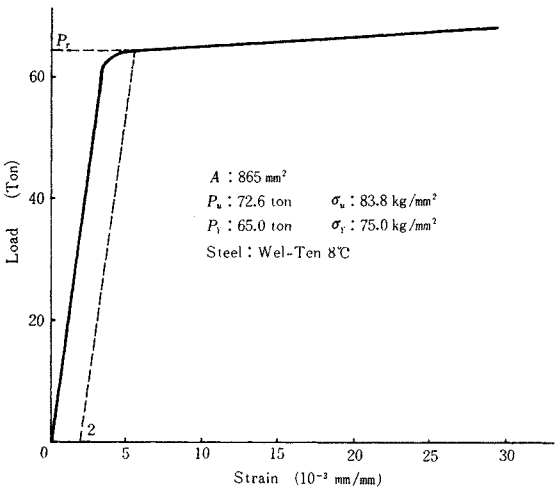

Fig. 8 Load-Strain Curve of the Test Material (Wel Ten 80 C).

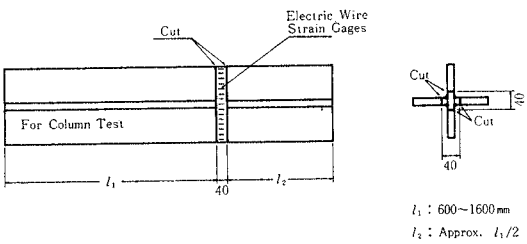

Fig. 9 Layout for Residual Stress Measurement.

distance from the ends as shown in Fig. 9. After taking the initial readings, the 40 mm wide section was sawed and then the four flanges were cut at their roots as shown in Fig. 9. The strain readings were then taken, when the cut-out pieces cooled down to room temperature. The difference before and after the cutting is a measure of residual strain. Fig. 10 shows the residual stress distributions thus obtained. The solid and broken lines show the residual stress patterns measured on both surfaces of the plates. As can be expected, the patterns show tensile residual stresses at the weld metal and its nearby area and at the flange tips; the latter is due to the flame cutting of the plate. Compressive residual stresses are present in the mid-portion. Contrary to previous measurements[18),20)] that the magnitude of the tensile residual stress at the weld metal is close to the yield stress of the material, the magnitude at and around the weld metal ranged from 15 to 40 kg/mm², which is far lower than the yield stress of around 75 kg/mm². This seems to be due to the particular method used here. As has been described, the cross section was sectioned at only four places so that complete release of the internal stress did not take place around the weld metal, where large variation of the stress did exist. A relatively large variation exists for residual stresses measured on both surfaces, especially for the columns with the smaller cross sections. The compressive residual stress distributed at the mid-portion of each flange was also variable; however, a tendency exists that the magnitude is larger for a smaller cross section. The approximate magnitudes of the average of compressive residual stresses ranged from 11 kg/mm² for the smallest cross section to 5 kg/mm² for the largest, which were around 15 percent and 7 percent of the yield stress, respectively.

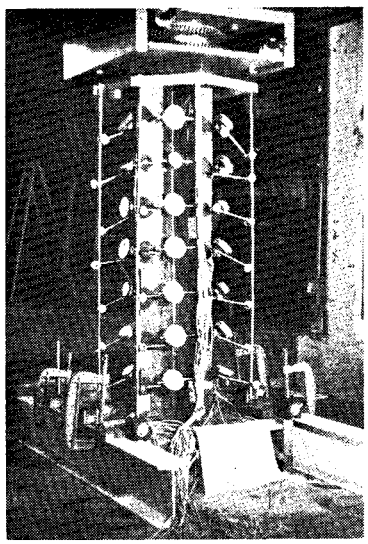

Fig. 11 Test Set-up.

The cruciform columns were tested in a 2 000 ton

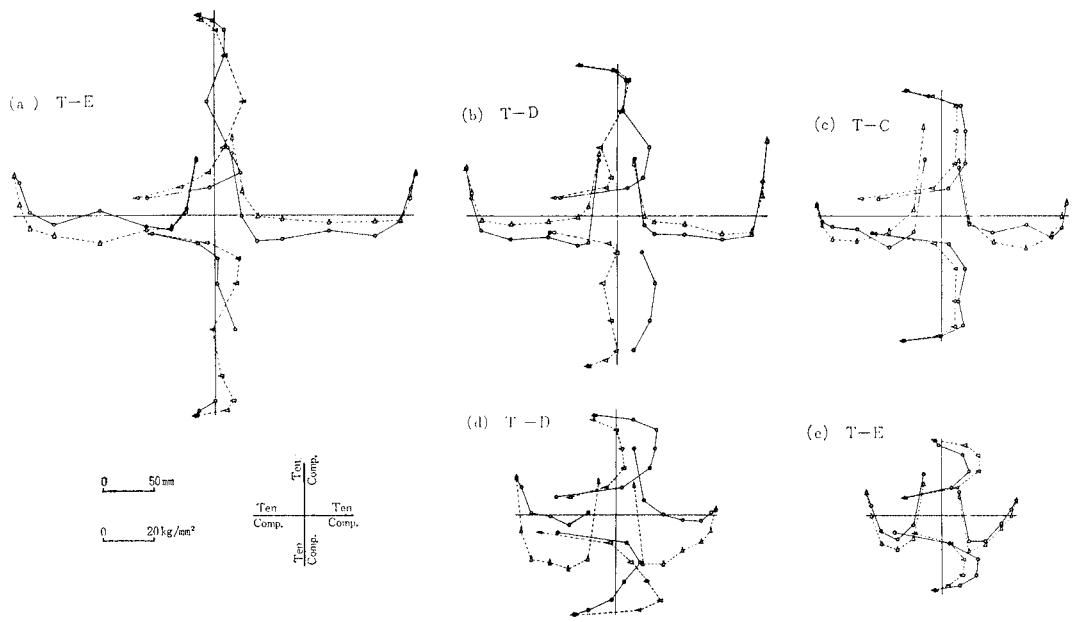

Fig. 10 Residual Stress Distribution.

universal testing machine. The ends of each specimen were milled flat. Two sets of discs were placed at both top and bottom of the specimens for alignment so that all four flanges could be loaded as uniformly as possible. The end condition of the columns is, therefore, close to that of a fixed end. The test set-up is shown in Fig. 11. The instrumentation consisted of electric strain gages placed at four flange tips at every quarter section of the column height, and a number of dial gages placed at the free edge of each flange at a certain interval along the height. The strain gages were used for alignment and to record the load-strain relationship, while the dial gages were to record the load-deflection relationship.

The load-mid-height strain relationships and the load-mid-height deflection relationships are shown in Figs. 12 and 13, respectively. The results of the buckling tests are summarized in Table 1. There are a number of methods proposed in determining the buckling load experimentally from the load-deflection relationship; however, for the tests of this study all methods tried resulted in buckling loads which were only two to four percent below the maximum loads, so that only the maximum loads are given in the table. The theoretical buckling loads obtained from Eq. 24 had to be multiplied by a correction factor to be more accurate. This is due to the assumptions in the analysis ; disregard of the warping rigidity and the deformation of the cross sections at the buckling[21]. The theoretical predictions given in Table 1 were the results thus corrected with the correction factor of 1.07 by Timoshenko[21], which is true for an elastic steel column free of residual stress, and employed here for the test columns as an approximation of the correction factor*.

As can be found in Table 1, the theoretical prediction suggests that no torsional buckling takes place before full yielding penetrates the cross section for columns T-A, T-B and T-C. The slenderness ratio of the test columns is about 20 taking one half of the column height as the effective length for flexural buckling. The columns with slenderness ratio of 20 made of 80 kg/mm² strength steel may fail by flexural instability before the full yielding loads of the cross section are reached or may exceed the yield loads. Consequently, it is possible that the width-

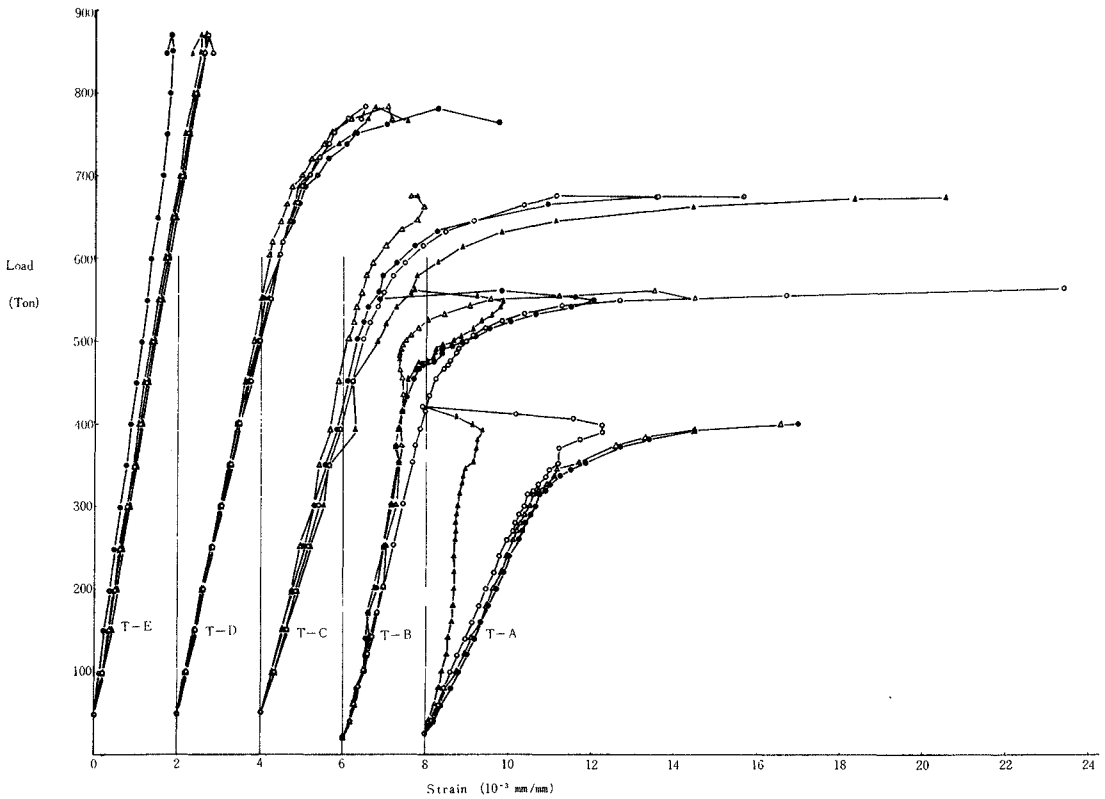

Fig. 12 Load-Mid-Height Strain Relation-Ship.

* The correction factor is not constant for columns with residual stresses and or yielded partially. The factor can be determined by comparing the results based on the analysis of this study and those obtained based on plate theory[15),24)].

thickness ratios of the columns TA, TB and TC are large enough to prevent torsional buckling and the columns fail by flexural buckling. As seen in Fig. 12, the four gages attached on four flange tips at mid-height showed similar relationships until the maximum loads were reached for columns T-D and T-E, while the strain readings at one or two gages started to decrease in the relationships of columns T-A, T-B snd T-C when the load-strain relationships deviated from the straight line and when the loads approached the ultimate loads; the tendency is more pronounced for columns with smaller cross sections. Since the strain gages were attached to the flange tips, the torsional buckling, which is actually plate bending, will not reduce the strain readings, and therefore the strain reversal indicates that the flexural buckling took place around the loading. The failure mode whether flexural buckling or torsional buckling can be more clearly determined from the load-deflection relationships of Fig.

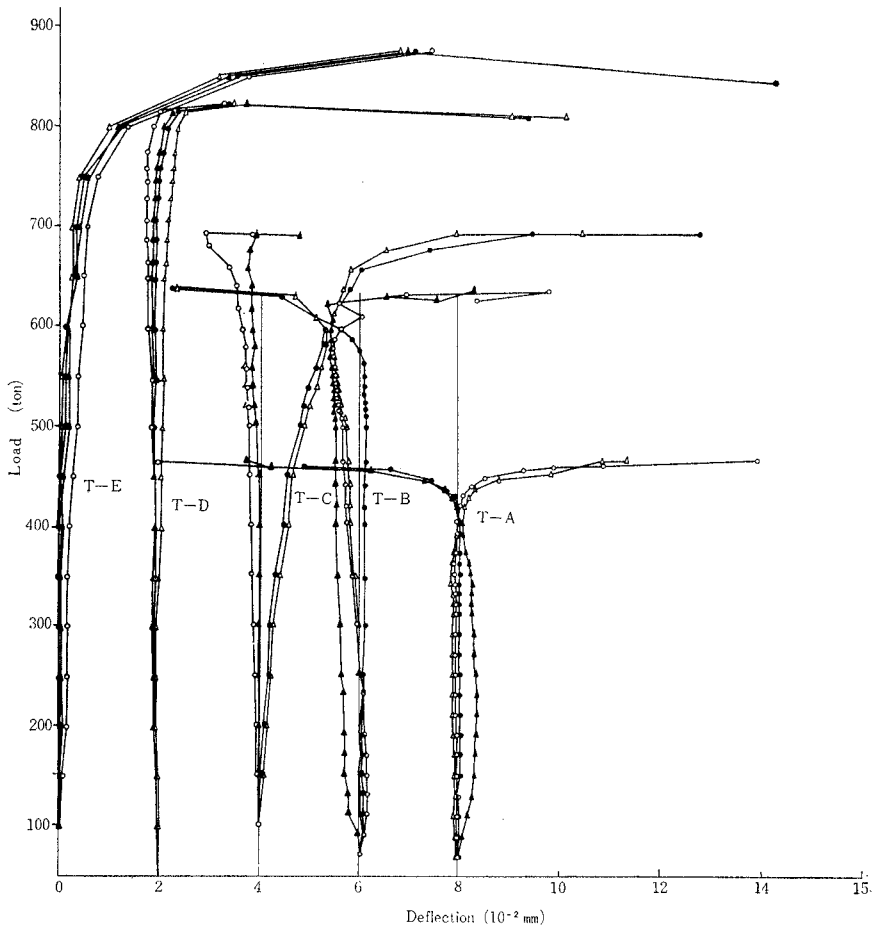

Fig. 13 Load-Mid-Height Deflection Relationship.

Table 1 Dimensions of Specimens and Summary of Test Results

Specimen No.	Dimension				Theoretical Prediction					Test Results	
					Yield Load	With Residual Stress			Without Residual Stress		
	L (mm)	b (mm)	t (mm)	b/t	P_Y (t)(1)	σ_{rc}/σ_Y	$P_{cr}{}^t/P_Y$(2)	$P_{cr}{}^i/P_Y$(2)	$P_{cr}{}^f/P_Y$(3)	P_{max} (t)	P_{max}/P_Y
T-A	600	77	17.1	4.5	378	0.15	1.0	1.0	1.0	413	1.09
T-B	801	103	17.2	6.0	515	0.12	1.0	1.0	1.0	546	1.06
T-C	1 000	127	17.2	7.4	642	0.11	1.0	1.0	1.0	670	1.04
T-D	1 200	154	17.2	9.0	780	0.08	0.97	1.0	1.0	778	0.99
T-E	1 600	199	17.3	11.5	1 030	0.06	0.78	0.78	0.90	846	0.82

(1) P_Y is the yield load determined as a product of cross sectional area multiplied by σ_Y=74.9 kg/mm².
(2) $P_{cr}{}^t$ $P_{cr}{}^i$ refer the torsional buckling loads based on the total and the incremental theories, respectively.
(3) $P_{cr}{}^f$ is the torsional buckling load of columns free of residual stress.

13. All four flanges moved in the same direction for columns T-D and T-E, suggesting the failures of the columns by torsional instability. The load-deflection relationship of the column T-C indicates that the flexural instability seemed to be dominant during the tests; however, when the ultimate load was approached, the mode of deflection changed and failed torsionally. The columns T-A and T-B, on the other hand, showed no clear tendency during the tests; however, a clear indication of flexural failure appeared when the loads were increased to the ultimate loads.

The experimentally obtained maximum loads are compared in Table 1 and are plotted in Fig. 7. The maximum loads of the columns with width-thickness ratios larger than 7.4, T-A, T-B and T-C, exceeded the yield loads of the cross sections as predicted. The column T-D with width-thickness ratio of 9 failed at a load nearly equal to the yield load. The incremental theory predicted no torsional buckling until the yield load is reached, while the total strain theory predicted a slightly lower load than the maximum load. As mentioned previously, the buckling load is slightly lower than the maximum load so that it may be concluded that a better correlation exists between the test result and the prediction based on the total strain theory. The column T-E with $b/t=11.5$, which failed instantaneously when a load of 82 percent of the yield load was applied and loading was stopped, also showed good agreement with the prediction for the effect of residual stress. Referring to the measured residual stress distribution of the column, the buckling seems to have taken place essentially in the elastic range; the analysis disregarding the presence of residual stress predicted a much higher load.

The current Japanese design specifications for steel highway bridges[25] limit the width-thickness ratio of outstanding flanges to be less than 12 and 17 for the main and the secondary members, respectively, made of steels of the yield stress up to 32 kg/mm². The limitation was specified based on the following equation[25] with buckling stress σ_{cr} equal to 95 percent of the yield stress

$$\frac{b}{t}\leqq\frac{80}{\sqrt{\sigma_{cr}}}=\frac{78}{\sqrt{\sigma_Y}} \quad \cdots\cdots(25)$$

where the unit of stress is in kg/mm². If Eq. 25 is extended to the test column with $\sigma_Y=75$ kg/mm², a width-thickness ratio of 9 results, which is in agreement with the test results of this experimental study. However, in a practical design of steel structures, it seems to be necessary to limit the width-thickness ratio to be smaller than the value thus determined so as to be able to add a safety margin for the torsional failure of an outstanding flange. The theoretically obtained ratio of 7.5 based on the total strain theory seems to be small enough to avoid premature failure and is recommended for the design of a member made of constructional alloy steel of 80 kg/mm² tensile strength.

5. SUMMARY AND CONCLUSIONS

This paper presents the results of an analysis of the torsional buckling strength of steel columns with particular emphasis on the effect of residual stress present prior to the application of loading. A numerical approach was used in evaluating the torsional stiffnesses of a cross section and other terms needed to be determined for the calculation of torsional buckling strength, so that columns with any patterns of residual stress distribution can be analysed. Numerical results in the form of column buckling curves are presented for columns of H and cruciform cross sections with idealized distributions of residual stress. The resulting column curves clearly show the effect of residual stress in the torsional buckling strengths. As opposed to flexural buckling, the elastic torsional buckling strength is affected by the presence of residual stress, which slightly raises or reduces the strength of H-columns depending on the cross sectional properties. A large reduction results, on the other hand, in the elastic-plastic torsional buckling strength due to the existence of residual stress. Of interest is the existence of a pinned-end column length for the buckling of cruciform columns; columns shorter than this length sustain the full yield load of the cross section and the failure of the column may be due to flexural instability.

A series of five welded built-up cruciform columns of constructional alloy steel with minimum yield strength of 70 kg/mm² have been tested to substantiate the theoretical results. The results of residual stress measurement show that the maximum magnitude of the compressive residual stress was relatively small with respect to the measured yield stress of 75 kg/mm² and ranged from 6 to 14 kg/mm² depending on the sizes of the cross sections. A comparison of buckling loads shows a good correlation between the theoretical results and the test results; for elastic-plastic buckling, the theoretical results based on the total strain theory gave a slightly lower load but one that was closer to the test result. The width-thickness ratio, with which premature failure of an outstanding flange can be avoided, turned out to be nine by the tests. However, to be safe in a practical design of a member made of constructional alloy steel of 80 kg/mm² tensile strength, the width-thickness ratio of 7.5 is recommended.

6. ACKNOWLEDGEMENTS

The theoretical part of the work described in this paper was a part of a dissertation presented to the Graduate Faculty of Lehigh University, Bethlehem,

Pennsylvania, U.S.A. The study was part of a research project on welded and rolled "T-1" steel columns sponsored by the U.S. Steel Corporation, and under the technical guidance of Task Group 1 of the Column Research Council.

The experiments were conducted at the Department of Civil Engineering, University of Tokyo, Tokyo, Japan. The investigation was sponsored by the Japan Railway Construction Public Corporation, under the technical direction of Dr. Jiro Tajima of the Japanese National Railways. The authors wish to thank Mr. Chin-Jung Ruo, a graduate student at the department, who performed the tests and compiled the data.

7. APPENDIX

7.1 Average Stress σ_i at Segment i

Strains at Edges	Average Stress $\frac{\sigma_i}{\sigma_Y}$
$\epsilon_i \geqq \epsilon_Y$, $\epsilon_{i-1} \geqq \epsilon_Y$	1
$\epsilon_i < \epsilon_Y$, $\epsilon_{i-1} < \epsilon_Y$	$\frac{\epsilon_i+\epsilon_{i-1}}{2\epsilon_Y}$
$\epsilon_i \geqq \epsilon_Y$, $\epsilon_{i-1} < \epsilon_Y$	$\frac{2\epsilon_i-\epsilon_{i-1}^2-1}{2\epsilon_Y(\epsilon_i-\epsilon_{i-1})}$
$\epsilon_i < \epsilon_Y$, $\epsilon_{i-1} \geqq \epsilon_Y$	$\frac{2\epsilon_{i-1}-\epsilon_i^2-1}{2\epsilon_Y(\epsilon_{i-1}-\epsilon_i)}$

7.2 Distance $X_{e,i}$ and Width $\Delta X_{e,i}$ of the Elastic Portion of the Segment i

Strains at Edges	$\Delta X_{e,i}$	X_e
$\epsilon_i \geqq \epsilon_Y$, $\epsilon_{i-1} \geqq \epsilon_Y$	0	—
$\epsilon_i < \epsilon_Y$, $\epsilon_{i-1} < \epsilon_Y$	ΔX	$\Delta X\left(i+\frac{1}{2}\right)$
$\epsilon_i \geqq \epsilon_Y$, $\epsilon_{i-1} < \epsilon_Y$	$\frac{\epsilon_i-1}{\epsilon_i-\epsilon_{i-1}}\Delta X$	$\Delta X(i-1)+\frac{\Delta X_{e,i}}{2}$
$\epsilon_i < \epsilon_Y$, $\epsilon_{i-1} \geqq \epsilon_Y$	$\frac{\epsilon_{i-1}-1}{\epsilon_{i-1}-\epsilon_i}\Delta X$	$\Delta X i-\frac{\Delta X_{e,i}}{2}$

where ΔX is the width of the Segments $\left(\Delta X=\frac{b}{2n}\right)$

7.3 K_i as defined in Eq. 20

Strains at Edges	K_i
$\epsilon_i \approx \epsilon_{i-1} \geqq \epsilon_Y$	$\frac{2+2\nu}{2+2\nu+\frac{3}{2}\left(\frac{\epsilon_i+\epsilon_{i-1}}{\epsilon_Y}-2\right)}$
$\epsilon_i \neq \epsilon_{i-1}$, $\epsilon_i \geqq \epsilon_Y$, $\epsilon_{i-1} \geqq \epsilon_Y$	$\frac{2+2\nu}{3\left(\frac{\epsilon_i-\epsilon_{i-1}}{\epsilon_Y}\right)}\log_e\frac{2+2\nu+3\left(\frac{\epsilon_i}{\epsilon_Y}-1\right)}{2+2\nu+3\left(\frac{\epsilon_{i-1}}{\epsilon_Y}-1\right)}$
$\epsilon_i < \epsilon_Y$, $\epsilon_{i-1} < \epsilon_Y$	1
$\epsilon_i \geqq \epsilon_Y$, $\epsilon_{i-1} < \epsilon_Y$	$\left(\frac{\epsilon_Y-\epsilon_{i-1}}{\epsilon_i-\epsilon_{i-1}}\right)+\left(\frac{2+2\nu}{3}\right)\left(\frac{\epsilon_Y}{\epsilon_i}\right)\left(\frac{\epsilon_i-\epsilon_Y}{\epsilon_i-\epsilon_{i-1}}\right)\cdot\log_e\left[\frac{2+2\nu+3(\epsilon_i/\epsilon_Y)}{2+2\nu}\right]$
$\epsilon_i < \epsilon_Y$, $\epsilon_{i-1} \geqq \epsilon_Y$	$\left(\frac{\epsilon_Y-\epsilon_i}{\epsilon_{i-1}-\epsilon_i}\right)+\left(\frac{2+2\nu}{3}\right)\left(\frac{\epsilon_Y}{\epsilon_{i-1}}\right)\left(\frac{\epsilon_{i-1}-\epsilon_Y}{\epsilon_{i-1}-\epsilon_i}\right)\cdot\log_e\left[\frac{2+2\nu+3(\epsilon_{i-1}/\epsilon_Y)}{2+2\nu}\right]$

7.4 q_i as defined in Eq. 22

Strain at Edges	q_i
$\epsilon_i \geqq \epsilon_Y$, $\epsilon_{i-1} \geqq \epsilon_Y$	$=\sigma_Y\left(i^2-i+\frac{1}{3}\right)$
$\epsilon_i < \epsilon_Y$, $\epsilon_{i-1} < \epsilon_Y$	$(\sigma_i-\sigma_{i-1})(i^3-1.5i^2+i-0.25)+[\sigma_{i-1}+(\sigma_{i-1}-\sigma_i)(i-1)]\left(i^2-i+\frac{1}{3}\right)$
$\epsilon_i \geqq \epsilon_Y$, $\epsilon_{i-1} < \epsilon_Y$	$(\sigma_Y-\sigma_{i-1})[(i-1)^3+1.5(i-1)^2\delta s_{e,i}+(i-1)\delta s_{e,i}^2+\frac{1}{4}\delta s_{e,i}^3]+[\sigma_{i-1}\delta s_{e,i}+(\sigma_{i-1}-\sigma_Y)(i-1)][(i-1)^2+(i-1)\delta s_{e,i}+\frac{1}{3}\delta s_{e,i}^2]+\sigma_Y\delta s_{p,i}[(i-\delta s_{p,i})^2+(i-\delta s_{p,i})\delta s_{p,i}+\frac{1}{3}\delta s_{p,i}^2]$
$\epsilon_i < \epsilon_Y$, $\epsilon_{i-1} \geqq \epsilon_Y$	$(\sigma_i-\sigma_Y)[(i-\delta_{e,i})^3+1.5(i-\delta s_{e,i})^2\delta s_{e,i}+(i-\delta s_{p,i})\delta s_{e,i}^2+\frac{1}{4}\delta s_{e,i}^3]+[\sigma_Y\delta s_{e,i}+(\sigma_Y-\sigma_i)(i-\delta s_{e,i})][(i-\delta s_{e,i})^2+(i-\delta s_{e,i})\delta s_{e,i}+\frac{1}{3}\delta s_{e,i}^2]+\sigma_Y\delta s_{e,i}[(i-1)^2+(i-1)\delta s_{p,i}+\frac{1}{3}\delta s_{p,i}^2]$

where $\delta s_{e,i}$ is the width of the elastic portion of the segment i divided by the width of the segment, and similarly. $\delta s_{p,i}$ is the non-dimensionalized width of the yielded portion.

8. REFERENCES

1) Bleich, F. : BUCKLING STRENGTH OF METAL STRUCTURES, McGraw-Hill, New York, 1952.
2) Stowell, E.Z. : A UNIFIED THEORY OF PLASTIC BUCKLING OF COLUMNS AND PLATES, NACA Rep. 898, 1948.
3) White, M.W. : THE LATERAL-TORSIONAL BUCKLING OF YIELDED STRUCTURAL STEEL MEMBERS, Ph. D. Dissertation, Lehigh University, 1956.
4) Galambos, T.V. : INELASTIC LATERAL BUCKLING OF BEAMS, Proc. of ASCE, Vol. 89, ST 5, October 1963.
5) Lee, G.C. : INELASTIC LATERAL INSTABILITY OF BEAMS AND THEIR BRACING REQUIREMENTS, Ph. D. Dissertation, Lehigh University, 1960.
6) Fukumoto, Y. and Galambos, T.V. : INELASTIC LATERAL-TORSIONAL BUCKLING OF BEAM-COLUMNS, Proc. of ASCE, Vol. 92, ST 2, April 1966.
7) Hoff, N.J. : APPROXIMATE ANALYSIS OF THE REDUCTION IN TORSIONAL RIGIDITY AND OF THE TORSIONAL BUCKLING OF SOLID WINGS UNDER THERMAL STRESS, Jour. Aero. Sci., Vol. 23, No. 6, June 1956.
8) Budiansky, B. and Mayers, J. : INFLUENCE OF AERODYNAMIC HEATING ON THE EFFECTIVE TORSIONAL STIFFNESS OF THIN WINGS, Jour. Aero. Sci., Vol. 23, No. 12, December 1956.

9) Kochanski, S.L. and Argyris, J.H. : SOME EFFECTS OF KINETIC HEATING ON THE STIFFNESS OF THIN WINGS, Aircraft Engineering, Vol. 29, No. 344, October 1957.
10) Fujita, J. : INFLUENCE OF RESIDUAL STRESSES ON THE INSTABILITY PROBLEMS, Jour. Zosen Kyokai, Japan, Vol. 107, July 1960. (Japanese with English Abstract.)
11) Lee, G.C. Fine, D.S. and Hastreiter, W.R. : INELASTIC TORSIONAL, BUCKLING OF H-COLUMNS Proc. of ASCE, Vol. 93, ST 5, Oct. 1967.
12) Ajmani., J.L. : DISCUSSION TO "INELASTIC TORSIONAL BUCKLING OF H-COLUMNS by Lee et al.", Proc. of ASCE, Vol. 94, ST3, March 1968.
13) Nishino, F. : DISCUSSION TO "INELASTIC TORSIONAL BUCKLING OF H-COLUMNS by Lee et al." Proc. of ASCE, Vol. 94, ST 6, June 1968.
14) Fukumoto, Y. and Ito, Y. : LOCAL BUCKLING STRENGTH OF OUTSTANDING FLANGES AND LIMITATION OF WIDTH-THICKNESS RATIO, Trans. JSCE, No. 160, December 1968 (In Japanese with English Abstract)
15) Nishino, F. : BUCKLING STRENGTH OF COLUMNS AND THEIR COMPONENT PLATES, Ph. D. Dissertation, Lehigh University, 1964.
16) Nishino, F. : BUCKLING OF COLUMNS, Jour of JSSC, Vol. 3, No. 16, April 1967 (In Japanese)
17) Beedle, L.S. and Tall, L. : BASIC COLUMN STRENGTH, Proc. of ASCE, Vol. 86, ST 7, July 1960.
18) Nagaraja Rao, N.R. and Tall, L. : RESIDUAL STRESSES IN WELDED SHAPES, Welding Jour., July 1964.
19) Odar, E., Nishino, F. and Tall, L. : RESIDUAL STRESSES IN ROLLED HEAT-TREATED T-1 SHAPES, Welding Research Council Bulletin, No. 121, April 1967.
20) Odar, E., Nishino, F. and Tall, L. : RESIDUAL STRESSES IN WELDED T-1 CONSTRUCTIONAL ALLOY STEEL SHAPES, Welding Research Council Bulletin, No. 121, April 1967.
21) Timoshenko, S. and Gere, J.M. : THEORY OF ELASTIC STABILITY, 2nd Ed., McGraw-Hill, New York, 1961.
22) Handelman, G.H. and Prager, W. : PLASTIC BUCKLING OF A RECTANGULAR PLATE UNDER EDGE THRUSTS, NACA Rep. 946, 1949.
23) Bijlaard, P.P. : THEORY AND TESTS ON THE PLASTIC STABILITY OF PLATES AND SHELLS, Jour. Aero. Sci., Vol. 16, No. 9, September 1949.
24) Nishino, F. and Tall, L. : RESIDUAL STRESS AND LOCAL BUCKLING STRENGTH OF STEEL COLUMNS, Fritz Engineering Laboratory Report 290. 11, Lehigh University, January 1967.
25) Japan Road Association : SPECIFICATIONS FOR STEEL HIGHWAY BRIDGES, Japan Road Association, July 1964 (In Japanese)

(Received July 12, 1968)